Target-in-the-loop Wavefront Sensing and Control with Collett-Wolf Beacon

Ernst Polnau
Intelligent Optics Laboratory, Institute for Systems Research, University of Maryland, 2107 Technology Ventures Building, College Park, Maryland 20742; e-mail: epolnau@mail.umd.edu

Mikhail A. Vorontsov
Intelligent Optics Laboratory, Computational and Information Sciences Directorate, U.S. Army Research Laboratory, 2800 Powder Mill Road, Adelphi, Maryland 20783 and Intelligent Optics Laboratory, Institute for Systems Research, University of Maryland, 2107 Technology Ventures Building, College Park, Maryland 20742; e-mail: mvorontsov@arl.army.mil

Abstract

It is well known that atmospheric turbulence can severely degrade performance of various optical systems including the laser beam projection systems discussed here. These systems are designed to create and maintain a laser spot of the smallest possible size on a remotely located object in the atmosphere. Compensation (mitigation) of turbulence effects in the laser beam projection systems is typically performed using adaptive optics (AO) wavefront correctors. In several applications the outgoing beam scattering off an extended object rough surface results in strong speckle modulation of the return wave. This speckle modulation is the major problem for the existing AO wavefront control techniques. In this paper we consider a new approach for speckle-effect mitigation in adaptive laser beam projection systems by creating an incoherent beacon (Collett-Wolf beacon) using either the projected beam itself or a single auxiliary laser illuminator beam. Using numerical simulations and bench-top experiment we show that using the Collett-Wolf beacon it is possible to mitigate speckle effects and achieve a high degree of turbulence compensation and increase of the laser beam brightness.

1. Introduction

Efficiency of laser beam projection through an optically inhomogeneous medium (most commonly atmosphere) onto an extended target with rough surface can be potentially improved using adaptive optics (AO) systems [1]. In these systems, control of the outgoing beam phase is based on sensing and pre-compensation of phase aberrations originating from random fluctuations of the propagation medium refractive index. Accurate sensing of phase aberrations requires existence of a small size (unresolved) light source or bright glint, known as a beacon that is located at the desired target aimpoint or at least in its vicinity. An ideal beacon represents a bright glint at the target aimpoint which scatters the outgoing or auxiliary (beacon) laser beam and thus results in formation of a backscattered spherical return wave propagating back to the transmitter aperture. In the monostatic beam projection system configuration considered, the receiver and transmitter apertures coincide. In the absence of such a bright glint – a common case for most practical applications - scattering of the projected beam off the target rough surface leads to formation of an in space randomly modulated backscattered optical field at the receiver plane, known as speckle-field [2]. Although, wavefront phase of the return speckle-field contains information on the medium-induced phase aberrations, direct extraction of this information from speckle-field phase measurements represents a complicated and still unresolved problem [3].

To bypass this problem, phase aberration sensing can be performed using an incoherent light source (beacon) that is created in air by focusing an auxiliary laser beam into a vicinity of the target (laser guide-star technique) [4]. One of the major drawback of this technique is that for propagation in a distributed (volume) phase distorting medium, the in practice unavoidable mismatch in the beacon (laser guide-star) and aimpont locations results in wavefront sensing errors. These errors cause decline in phase aberration compensation efficiency associated commonly with anisoplanatism [5].

2. Experimental demonstration

2.1. Experimental setup

In this paper we show that sensing of the propagation medium-induced phase aberrations for AO control can be achieved by creating a target-surface beacon by means of rapid angular scanning of either the outgoing or an auxiliary (beacon) laser beam. The beam scanning results in the continuous movement of the projected beam footprint (target hit spot) at the target surface within a target area containing the aimpoint. For simplicity we assume here a periodic scanning with the period T_{scan} that is smaller than the characteristic time τ_{at} of the propagation medium (atmosphere) change ($T_{scan}<\tau_{at}$).

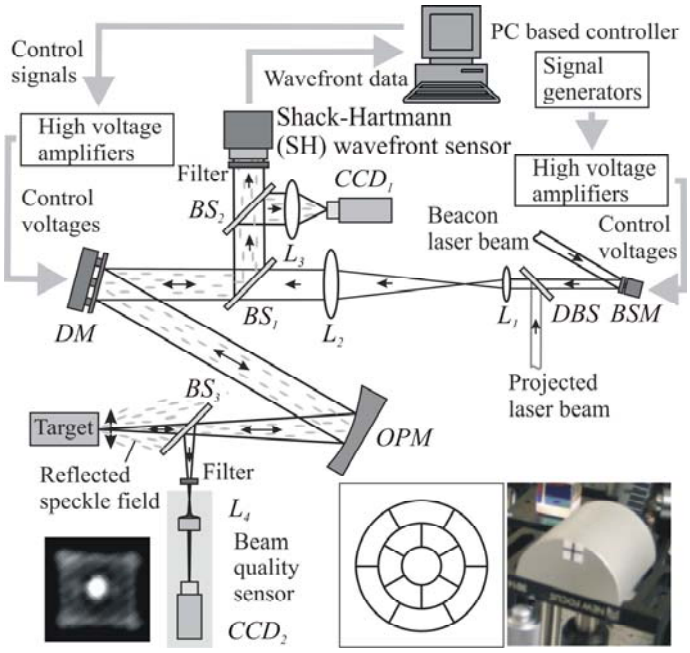

Fig.1. Scheme of the experimental setup used for closed loop experiments using SA PC and conventional PC. The image on the left is taken with the beam quality sensor where the scanning beacon laser and the laser spot of the projecting laser can be seen. The side length of the image corresponds to 120 micron. The two photos on the right show the 13-channel

The target hit-spot movement produces similar effect on the wave scattered off the target surface as does a thin moving diffuser on non-scanning laser beam with identical intensity distribution. Note that a moving diffuser with an entering laser beam is known as the Collett-Wolf light source (see for example ref [6]). Similarly we use term the Collett-Wolf (CW) beacon that is applied here to the long-exposure hit-spot intensity distribution that is integrated over the scanning period T_{scan}. Correspondingly the effective size of the CW beacon b_{CW} depends on both the characteristic size of the target hit spot b_s and the amplitude of scanning b_{scan}.

Since the hit-spot movement leads to update of the speckle-field patterns inside the transceiver aperture, the characteristic time of the speckle pattern update τ_s can be made significantly smaller than the integration time τ_{pr} of the wavefront sensor photo-receiver ($\tau_s<<\tau_{pr}$). This leads to time-averaging of multiple speckle-field realizations, achieved prior to any significant variation in both the propagation medium optical inhomogeneities and AO wavefront phase shaping. Assume that the speckle-average data are obtained using a wavefront sensor with the integration time $\tau_{pr}<<\tau_{AO}<\tau_{at}$, where τ_{AO} is the characteristic time of AO system response. The function $\Phi(\mathbf{r})$ reconstructed from these data is referred to here as the speckle-average (SA) phase. Here $\mathbf{r}=\{x,y\}$ is the coordinate vector in the transceiver pupil

plane. In the experiments described we used a conventional Shack-Hartmann (SH) wavefront sensor and correspondingly the SA phase $\Phi(\mathbf{r})$ was reconstructed from measurements of the speckle-average wavefront slopes.

The CW beacon was created using an auxiliary beam (beacon beam with wavelength λ_b=0.532 μm) that propagated through the same optical train as the principle laser beam (wavelength λ_p=0.63 μm). Both beams were projected onto an extended target as shown in Fig. 1 and had approximately equal diameter (10 mm) and power (10 mW) in the optical system input plane. Prior to entering the system the beacon beam was reflected from a wavefront corrector (beam steering mirror BSM) used for small amplitude (1.2 mrad) periodic scanning of its propagation direction. To distinguish these two laser beams we use the terms scanning or beacon beam and non-scanning or projected beam. Both beams were combined using a dichroic beam-splitter *DBS* in the system input. The optical relay system with 2.5 magnification factor (lenses L_1 and L_2 with the focal lengths 200 mm and 500 mm correspondingly) reimaged the beam steering mirror to the deformable mirror (*DM*). The deformable mirror (25 mm aperture) was made from a semipassive bimorph element with 13 electrodes that are shown schematically on inset in Fig. 1. This mirror was used for both insertion and adaptive compensation of phase aberrations. The beacon and principle projected beams were further reflected from an off-axis parabolic mirror (*OPM*) with a focal length of 381 mm and focused onto the plane front side of an aluminum half cylinder of radius 50 mm (see inset in Fig. 1). Light scattering off the target surface roughness resulted in formation of the propagating back speckle fields that entered both the SH wavefront sensor (Wavefront Sciences CLAS 2-D) and the imaging system. A narrowband optical filter in the SH wavefront sensor pupil plane blocked the projected beam. Correspondingly wavefront sensing was only performed using the speckle field originating from the beacon beam.

The imaging system was composed of lens L_3 and a camera (CCD_1) located in the image plane of the target. Example of a superimposed image of the target hit spot formed by the projected beam, and an image of the square shape CW beacon (long-exposure image of the scanning beam) as registered by this camera is shown on inset (left bottom corner).

Scanning of the beacon beam was achieved using the beam steering mirror *BSM* by applying harmonic control signals with frequencies of 800 Hz and 750 Hz to x- and y- actuators of the *BSM*. The size of the CW beacon b_{scan} was controlled by changing the amplitude v_{scan} of the applied signals ranging from b_{scan} = 0.25 b^{dif} bdif to b_{scan} = 20.0 b^{dif}, where b^{dif} is the diffraction limited hit-spot diameter of approximately 25 microns for the beacon laser. The period of 2D scanning of the beacon beam lasted T_{scan} = 20 msec. This time was significantly smaller than both the imaging camera integration time τ_{CCD} = 33 msec and the integration time τ_{pr} = 128 ms of a camera in the SH wavefront sensor.

The SH sensor was used to measure either the speckle-averaged or instantaneous wavefront slopes of the return beacon wave. The instantaneous phase slopes were obtained using the non-scanning beacon beam (b_{scan}= 0). The standard computational routines were used for: (a) reconstruction of both the speckle-average $\Phi(\mathbf{r})$ and instantaneous $\varphi(\mathbf{r})$ phase functions from slopes; (b) calculation of the corresponding aberration coefficients $\{a_j^{\Phi}\}$ and $\{a_j^{\varphi}\}$ obtained by deconvolution of functions $\Phi(\mathbf{r})$ and $\varphi(\mathbf{r})$ over the deformable mirror response functions $\{S_j(\mathbf{r})\}$, (j=1,…,13); (c) calculation of the Strehl ratio *St* and root-mean-square (*RMS*) phase error ε for the speckle-average and instantaneous phase respectively.

For evaluation of AO compensation performance independent of the SH sensor, we used the beam quality sensor composed of a microscope-objective (lens L_4) with camera (CCD_2). This sensor provided observation and measurement of the magnified images (with magnification factor 10) of target plane intensity distributions for both the principle and the beacon beams.

For AO control of the deformable mirror (*DM*) shape, we used conventional approach based on phase conjugation principle, so that the control signal (voltages) $\{u_j\}$ applied to the *DM* electrodes were set to cancel the obtained from wavefront sensing aberration coefficients $\{a_j^{\Phi}\}$or $\{a_j^{\varphi}\}$. Note that for extended targets AO compensation of phase aberrations is an iterative process [7]. Correspondingly the phase-conjugate phase aberration compensation leads to the following control iterative procedures of the control voltages update used in the experiments:

$u_j(n+1) = -a_j^{\Phi}(n)$ for AO control based on SA phase, and $u_j(n+1) = -a_j^{\varphi}(n)$ for the instantaneous phase aberration compensation, where n=1,…,N is the iteration number, and N is the total number of iterations. To distinguish these two control rules the first control signal update algorithm is referred to here as the speckle-average phase conjugation (SA PC) and the second as conventional PC algorithm.

2.2. Experiments and results

The following AO compensation experiments, referred to here as the adaptation trials, were performed using the beacon beam with scanning amplitude b_{scan} for SA PC and b_{scan} = 0 for PC based control. At the beginning of each adaptation trial a set of random voltages $\{u_j(n=0)\}$, (j=1,…,13) were applied to the deformable mirror electrodes thus generating an initial phase aberration in the system optical train. Note that the initial (n=0) aberration was identical for both SA PC and PC control. The aberration compensation included N=10 iterations of either SA PC or PC control algorithms. The following characteristics of the adaptation process were recorded during these iterations: Strehl ratio $St(n)$), residual phase error $\varepsilon(n)$ intensity distributions of the principle beam in the target plane $I_n(\mathbf{r})$, and both SA and instantaneous phase functions.

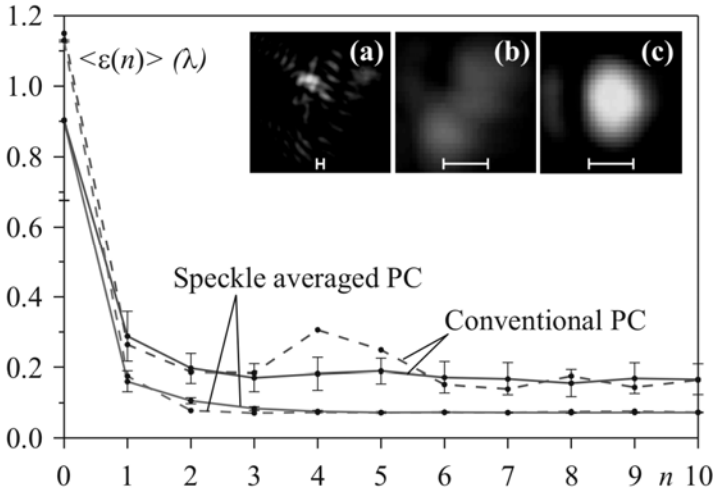

Fig.2. averaged phase error characteristics $<\varepsilon(n)>$ vs. number of optimization steps (n) for scanning (Speckle Averaged PC) and non-scanning (Conventional PC) optimization trials. The solid lines represent the averages of 20 optimization trials with different random start settings of the deformable mirror. For each case, PC as well as SA PC, also a typical single optimization trial represented by the dashed lines is shown. The inserts show images of the projected laser spot taken with the beam quality sensor. (a) after introduction of aberrations before any optimization was performed, (b) after optimization with conventional PC (averaged over optimization steps 6 to 10), (c) after optimization with SA PC (averaged over optimization steps 6 to 10). The length of the white bar in each image corresponds to 25 microns. The intensity in image (a) is ten times amplified compared to the two other images (b) and (c)

Fig. 2 illustrates AO system performance for typical SA PC and PC adaptation trials. The averaged phase error characteristics $<\varepsilon(n)>$ (adaptation curves) for SA PC and PC control obtained using 20 statistically independent random phase aberration functions are also presented in Fig. 2. As clearly seen the SA PC control based on the Collett-Wolf beacon generated by using 2D beam scanning, resulted in significantly better performance than the conventional PC compensation technique based on the non-scanning beacon beam. Indeed, the SA PC control resulted in significantly faster convergence, and smaller both the residual phase error $<\varepsilon(N)>$ and its standard deviation (indicated in Fig. 2 by vertical bars) that characterizes stability (robustness) of the AO process convergence. The efficiency of SA PC phase aberration compensation is also illustrated by the target-plane averaged intensity distributions in Fig. 2 which were obtained prior to adaptation (a), with PC (b) and with SA PC (c) compensation. Images of the pattern attached to the target surface (a piece of paper with printed number and horizontal and vertical lines) obtained prior to adaptation (a) and with SA PC (b) in illustrated in Fig. 3. The target plane intensity distributions in Fig. 2 were recorded using the hit-spot sensor (lens L_4 and camera CCD_2), while the images in Fig. 3 were captured using the imaging sensor (lens L_3 and camera CCD_1) in Fig. 1.

Consider dependence of the SA PC compensation efficiency on the shape and size of the Collett-Wolf beacon. In the experiments we used the Collett-Wolf beacon in the form of a line and square obtained using correspondingly one- and two-dimensional scanning of the beacon beam. For a fixed amplitude of one- or two-dimensional scanning the SA PC adaptation trial containing N=10 iterations each, was repeated ten times. For each adaptation trial we used different realizations of both phase aberrations and target surface roughness. The change in the target surface roughness was achieved using an orthogonal to optical axis displacement of the target (aluminum cylinder in Fig. 1) at the distance exceeding the hit-spot size. The dependence of the averaged SA PC compensation efficiency for one- and two-dimensional scanning are shown in Fig. 4. In both cases the average Strehl ratio increases as scanning amplitudes increases until a maximum is reached. This maximum is reached for a scanning amplitude of two times the size of the diffraction limited laser spot size b^{dif} for one-dimensional scanning and four times the size of the diffraction limited laser spot size for two-dimensional scanning. For higher scanning amplitudes the performance of SA PC decreases faster for one-dimensional scanning than for two-dimensional scanning. The reason is probably a combination of two factors which lead to increased instability of the control loop in particular for one-dimensional scanning with large amplitudes. Firstly, larger scanning amplitudes lead to larger errors in the measured wavefront due to anisoplanatism. Secondly, in the case of one-dimensional scanning even a relatively small tilt perpendicular to the scanning direction, introduced during subsequent iterations has the effect, that a completely different path of the surface is scanned.

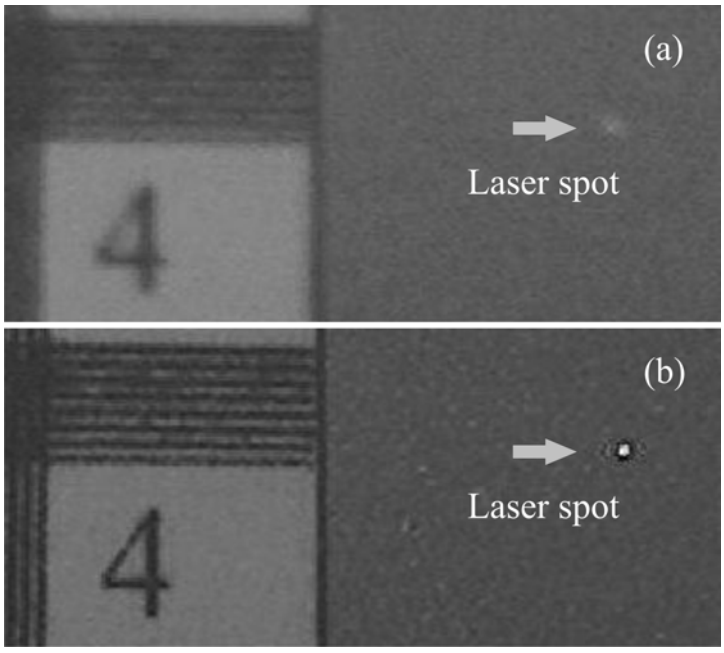

Fig.3. Images taken with the target imaging camera CCD_1 after introduction of random aberrations: (a) before optimization, (b) after optimization with SA PC.

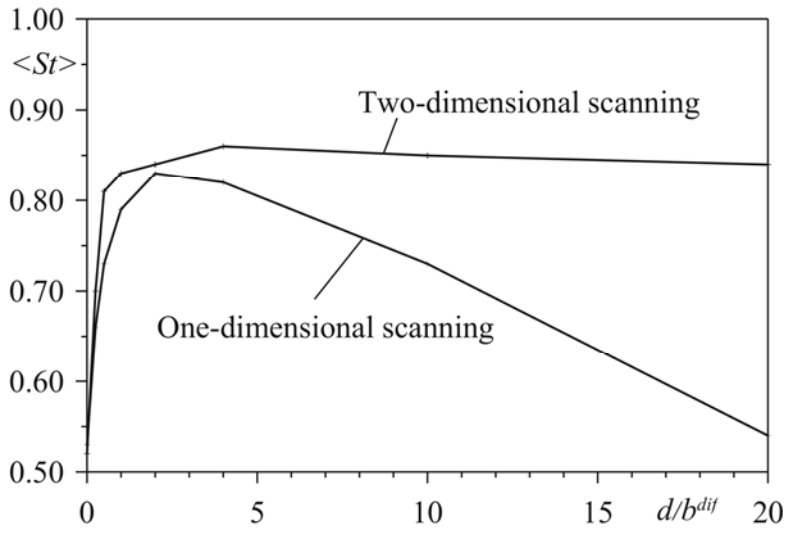

Fig.3. Dependence of the optimized Strehl ratios on the normalized scanning amplitude d/b^{dif} for one-dimensional and two-dimensional scanning.

3. Conclusions

In conclusion, we have demonstrated that SA PC adaptive optics can effectively bypass the problems associated with speckle fields from the rough surface of the target. In particular SA PC is capable to provide a stable closed loop control for an adaptive optics system with a phase aberration compensation efficiency that is superior to conventional PC for cases where the efficiency of the later is reduced by the presence of speckle patterns in the radiation reflected from the target surface.

4. REFERENCES

1. Primmerman C.A., Price T.R., Humpreys R.A., Zollars B.G., Barclay H.T., and Herrmann J., Atmospheric-compensation experiments in strong-scintillation conditions, Applied Optics, Vol. 34, 2081-2088, 1995
2. Goodman J.W., *Statistical Optics,* Wiley, 1985
3. Vorontsov M.A., Kolosov V.V., Target-in-the-loop beam control: basic considerations for analysis and wave-front sensing, J. Opt.Soc.Am.A, Vol. 22, 126-140, 2005
4. Roggemann M.C., Welsh B., *Imaging Through Turbulence,* CRC Press, 1996
5. Vorontsov M.A., Kolosov V.V., Polnau E., Target-in-the-Loop Wavefront Sensing and Control with a Collet-Wolf Beacon: Speckle-Average Phase Conjugation, Applied Optics, to be published (2008).
6. Collet E., Wolf W., Is complete coherence necessary for the generation of highly directional light beams? Optics Letters, Vol. 2, 27-29, 1978
7. Vorontsov M.A., Kolosov, V.V, Kohnle A., Adaptive laser beam propagation on an extended target: phase- and field-conjugate pre-compensation, JOSA A, Vol. 24, 1975-1993, 2007